Extension of the approximate 3D-RISM-KH molecular solvation theory to liquid aniline and pyridines

Roy, Dipankar; Kovalenko, Andriy

Publisher's version / Version de l'éditeur:
https://doi.org/10.1016/j.rechem.2022.100365
Results in Chemistry, 4, C, 2022-01

Results in Chemistry 4 (2022) 100365

Contents lists available at ScienceDirect

Results in Chemistry

journal homepage: www.sciencedirect.com/journal/results-in-chemistry

Extension of the approximate 3D-RISM-KH molecular solvation theory to liquid aniline and pyridines

Dipankar Roy [a], Andriy Kovalenko [a,b,*]

[a] Departments of Biological Sciences, University of Alberta, CW 405, Biological Sciences Bldg., Edmonton, Alberta T6G 2E9, Canada
[b] Nanotechnology Research Centre, National Research Council of Canada, 11421 Saskatchewan Drive, Edmonton, Alberta T6G 2M9, Canada

ARTICLE INFO

Keywords:
Aromatic Amines
Molecular Solvation Theory
Reference Interaction Site Model
Molecular Dynamics
Solvation Free Energy
Density Functional Theory
π-stacking Interactions

ABSTRACT

Four liquid aromatic nitrogen-containing compounds, viz. aniline, pyridine, 2-methylpyridine, and 2,6-dimethylpyridine, were analyzed with molecular dynamics simulations, three-dimensional reference interaction site model, and density functional theory calculations. These liquids are found to have multimeric ordered structures stabilized by π-stacking and C-H•••π interactions. The solutes solvation free energy computed with the reference interaction site model is in good agreement with the experimental results, and performs better than the conductor like polarizable continuum model used in electronic structure calculation.

Introduction

Liquid aromatic amines and N-containing heterocycles are important class of compounds with vast use in synthetic chemistry as starting chemicals, pharmaceutical applications, drug design, industrial applications as solvents, etc. For instance, aniline is used in making dyes, rubber chemicals, drugs, explosives, plastics, and photographic materials. The pyridines are important heterocyclic compounds will applications in drugs and pharmaceutical industry. The parent molecule, pyridine is the most commonly used infrared (IR) probe for measuring protonic acidity according to the ion-pair method. The pyridine and methyl-pyridines (2-Methyl pyridine [2-picoline], 2,6-Dimethylpyridine [Lutidine]) are strong bases. The structures of liquid aromatic amines were subject to molecular simulation and diffraction studies, both in neat liquid form as well as in hydrated conditions [1–6]. The crystal structure of aniline was to have N-H•••π and N-H•••N hydrogen bonds, obtained under special conditions [7]. The crystal structures of pyridine showed stacking interactions and C-H•••π interactions [8,9]. The solid structures of 2-Methyl and 2,6-Dimetylpyridines were also reported to have stacked and C-H•••π interactions [10,11]. The herring-bone type arrangements in crystal of 2-Methylpyridine grown in situ from liquid were reported to have directional C-H•••N directional H-bonds [10]. The macroscopically polar crystals of 2,6-Dimethylpyridine are arranged in one-dimensional chains arranged in a planer way by H-bonds [11]. A comparison of the reported liquid and solid structures of these four aromatic amines points to probable ordered arrangement in the liquid form stabilized via X-H•••π and/or H-bonding interactions as well as π-stacking. In this work, we have used state-of-the-art computational methods to examine the liquid states of the four aromatic compounds (Fig. 1) to provide a better understanding of the molecular nature of the liquid state and the molecular interactions involved. We have employed all-atom molecular dynamics (MD) simulations, three-dimensional reference interaction site model (3D-RISM), and dispersion corrected density functional theory (DFT) toward this exercise.

The theoretical framework of RISM was introduced by Chandler and coworkers. Detailed theoretical derivations behind the RISM formalism were provided elsewhere [12–18]. Here we briefly describe the key concepts involved. The 3D-RISM theory provides probability density of all possible interaction sites γ of solvent molecules around a solute of arbitrary shape at position $\boldsymbol{r}$ as a product of the average number density ρ_γ in the bulk solution and the normalized density distribution $g_\gamma(\boldsymbol{r})$. The total correlation function $h_\gamma(\boldsymbol{r})$ is obtained from the direct correlation function $c_\gamma(\boldsymbol{r})$ and the site-site bulk susceptibility function χ for α solvent sites around a solute such as:

$$h_\gamma(\boldsymbol{r}) = \sum_\alpha \int d\boldsymbol{r}' c_\alpha(\boldsymbol{r}-\boldsymbol{r}')\chi_{\alpha\gamma}(r')$$

The direct correlation function is expressed at temperature T as: $c_\gamma(\boldsymbol{r}) \sim -u_\gamma(\boldsymbol{r})/(k_B T)$, where k_B is the Boltzmann constant. The bulk susceptibility function χ is an input into the 3D-RISM integral equation, and the

* Corresponding author.
E-mail address: andriy.kovalenko@ualberta.ca (A. Kovalenko).

https://doi.org/10.1016/j.rechem.2022.100365
Received 18 March 2022; Accepted 8 May 2022
Available online 13 May 2022

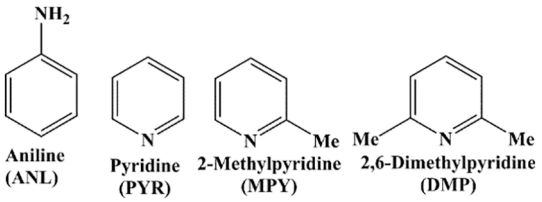

Fig. 1. Liquid aromatic amines studied for molecular simulations.

Table 1
Force field parameters used in the RISM simulations.

Atom Type	Mass (amu)	σ (Å)	ε (kcal/mol)
N	14.007	3.250	0.170
$C_{aromatic}$	12.006	3.399	0.086
C[H_3]	15.036	3.667	0.1494
$H_{aromatic}$	1.008	2.599	0.015
H	1.008	1.069	0.0157

Table 2
MD simulated and reference densities (ρ in gm/cm^3) of aromatics used in this study at 298 K.

Molecule	ρ(MD)[a]	ρ(Reference)[b]	ε^c
Aniline	1.036 (±0.036)	1.0217 (47)	6.8882
Pyridine	0.985 (±0.004)	0.98272 (48)	12.978
2-Methylpyridine	0.940 (±0.003)	0.9443 (47)	9.9533
2,6-Dimethylpyridine	0.917 (±0.006)	0.9252 (48)	7.1735

[a]Error estimates in calculation are provided in the parentheses. [b]References are cited in the parentheses. [c]Dielectric constant used for the RISM calculations.

dielectrically consistent RISM (DRISM) formalism is used to construct it from the intramolecular correlation function ($\omega_{\alpha\gamma}$). The site-site susceptibility function has intra- and inter-species parts:.$\chi_{\alpha\gamma}(r) = \omega_{\alpha\gamma}(r) + \rho_\alpha h_{\alpha\gamma}(r)$

The intramolecular term for rigid species with site separation $l_{\alpha\gamma}$ is expressed in the reciprocal k-space in terms of the zeroth-order spherical Bessel function $j_0(x)$ as:.$\omega_{\alpha\gamma}(r) = j_0(kl_{\alpha\gamma})$

The interspecies radial total correlation function between sites α and γ for all the sites on all the species in liquid medium is given by the $h_{\alpha\gamma}(r)$ term. In a 3D-RISM calculation, the total correlation function involving all the species (present in the solution) can be expressed as via DRISM formalism with renormalized inter and intramolecular parts:

$$\widetilde{h}_{\alpha\gamma}(r) = \widetilde{\omega}_{\alpha\mu}(r)*c_{\mu\nu}(r)*\widetilde{\omega}_{\nu\gamma}(r) + \widetilde{\omega}_{\alpha\mu}(r)*c_{\mu\nu}(r)*\rho_\nu\widetilde{h}_{\nu\gamma}(r)$$

$$\widetilde{\omega}_{\alpha\gamma}(r) = \omega_{\alpha\gamma}(r) + \rho_\alpha\chi_{\alpha\gamma}(r)$$

$$\widetilde{h}_{\alpha\gamma}(r) = h_{\alpha\gamma}(r) - \chi_{\alpha\gamma}(r)$$

The 3D interaction potential of the solute acting on solvent site γ, $u_\gamma(\boldsymbol{r})$, is given by the sum of the pairwise site-site potentials from all the solute interaction sites i located at $\boldsymbol{r}_i$ as: $u_\gamma(\boldsymbol{r}) = \sum_i u_{i\gamma}(|\boldsymbol{r} - \boldsymbol{r}_i|)$.

To obtain the path independent chemical potential, a closure relation is required which imposes a set of consistency conditions. A closure relation is a mathematical approximation that helps integrating an infinite chain of interactions involving intra- and inter-molecular sites. In this study, we have used the well-established Kovalenko-Hirata closure relation for RISM calculations [19]. The functional form of the KH closure is given as:

$$g_\gamma(\boldsymbol{r}) = \begin{cases} exp\left(-u_\gamma(\boldsymbol{r})/(k_B T) + h_\gamma(\boldsymbol{r}) - c_\gamma(\boldsymbol{r})\right) & \text{for} \quad g_\gamma(\boldsymbol{r}) \le 1 \\ 1 - u_\gamma(\boldsymbol{r})/(k_B T) + h_\gamma(\boldsymbol{r}) - c_\gamma(\boldsymbol{r}) & \text{for} \quad g_\gamma(\boldsymbol{r}) > 1 \end{cases}$$

where k_B is the Boltzmann constant and T is temperature in Kelvins.

The excess chemical potential is obtained in a closed analytical form with the Heaviside step function (Θ) as:

$$\mu_{solv} = \sum_\gamma \int_V d\boldsymbol{r}\Phi_\gamma(\boldsymbol{r}) \quad \text{and} \quad \Phi_\gamma\left(\boldsymbol{r}\right)$$
$$= \rho_\gamma \quad k_B T\left[\frac{1}{2}h_\gamma{}^2\left(r\right)\Theta\left(-h_\gamma\left(r\right)\right) - c_\gamma\left(r\right) - \frac{1}{2}h_\gamma\left(r\right)c_\gamma\left(r\right)\right]$$

Another important parameter, partial molar volume (PMV, $\bar{V}$) of a solute can be obtained by extending the RISM formalism with the

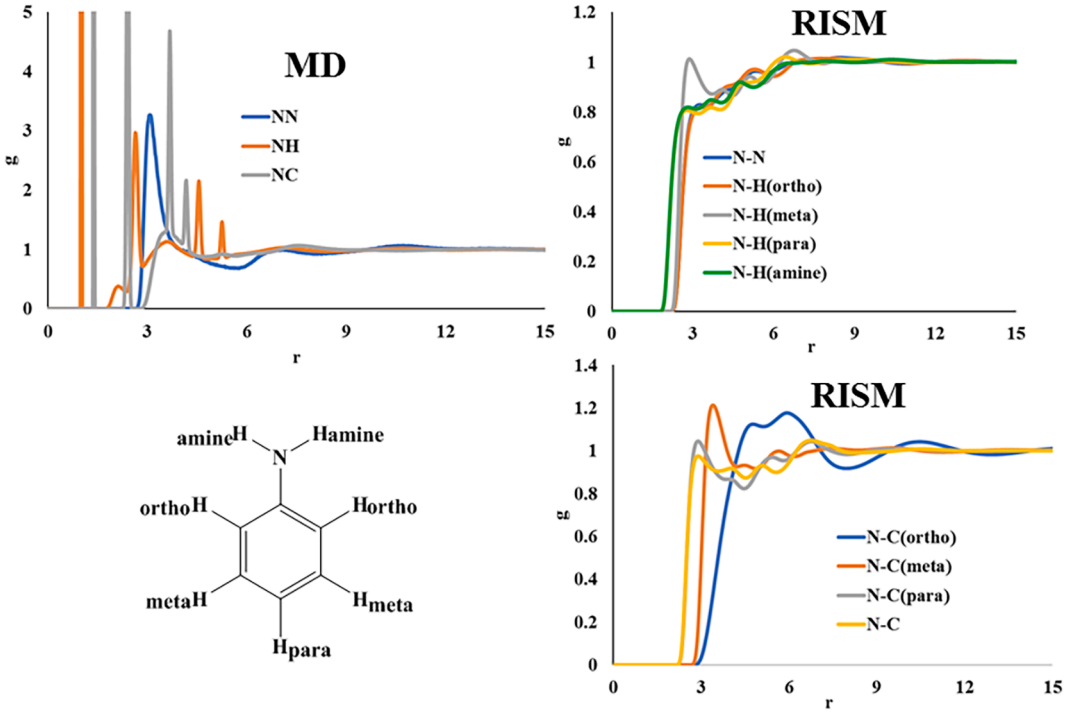

Fig. 2. Radial distribution function (rdf, MD) and pair distribution (pdf, RISM-KH) plots of liquid aniline.

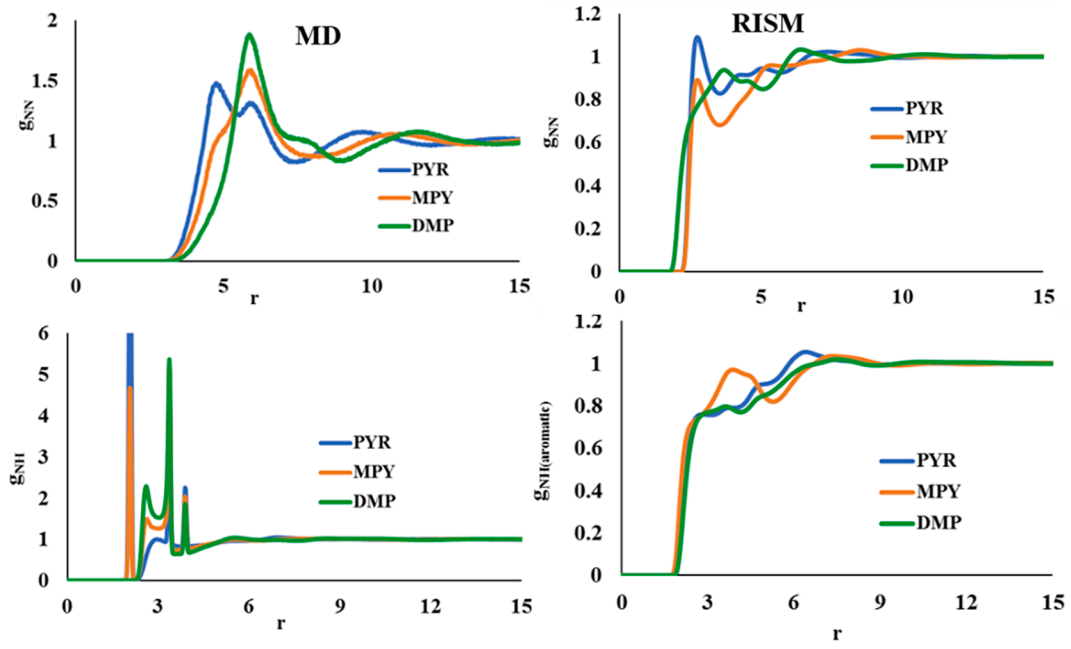

Fig. 3. Ring-nitrogen radial distribution function (rdf, MD) and pair distribution (pdf, RISM-KH) plot of liquid pyridine (PYR), 2-Methylpyridine (MPY), and 2,6-Dimethylpyridine (DMP).

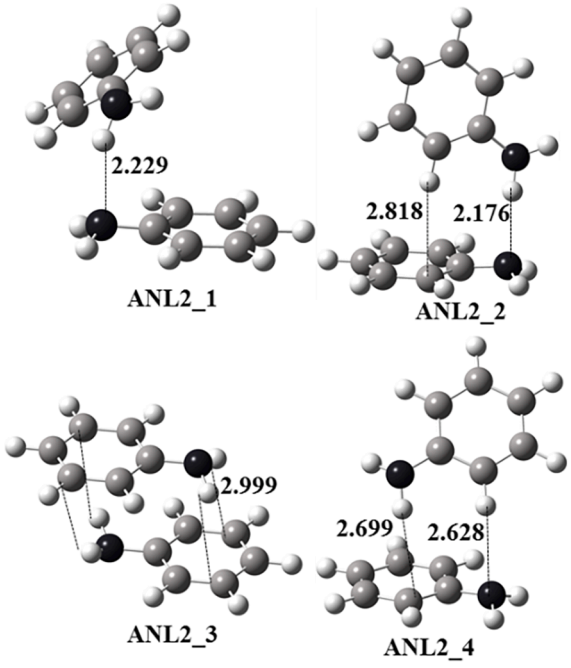

Fig. 4. SMD/B3LYP-D3/cc-pVTZ optimized geometries of top four dimers of aniline (ANL). Interatomic distances are in Å. Atom color code: C, grey; H, white; N, black.

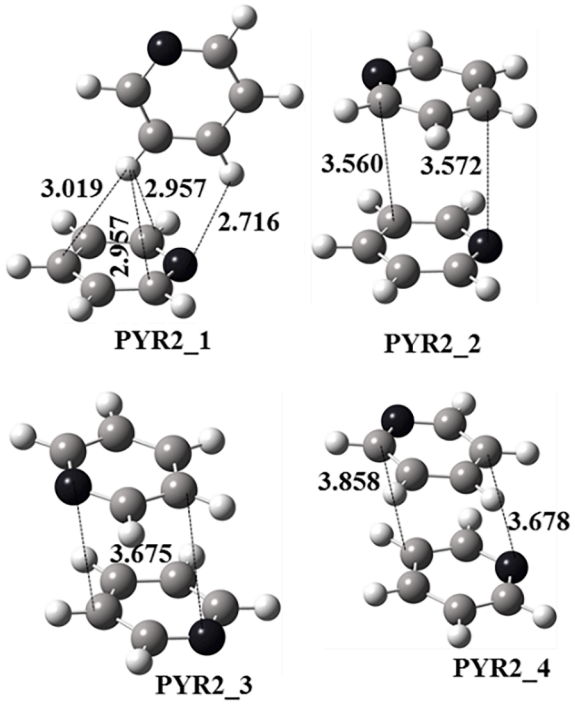

Fig. 5. SMD/B3LYP-D3/cc-pVTZ optimized geometries of top four dimers of pyridine (PYR). Interatomic distances are in Å. Atom color code: C, grey; H, white; N, black.

Kirkwood-Buff theory as:

$$V = \mathrm{k_B} T \chi_T \left(1 - \sum_{\gamma} \rho_{\gamma} \int dr\ c_{\gamma}(r)\right)$$

where χ_T is the isothermal compressibility. A negative PMV points to local reduction in volume around solute, the situation often found around a charged ion in polar (protic) solvents.

The RISM computed excess chemical potentials are qualitative in nature when used as an absolute measure of solvation free energy. The error comes from the theoretical artifacts in wrong internal pressure calculations, inadequacy of the use of force field parameters, etc. One way to correct the excess chemical potentials is the so-called "universal correction" (UC) scheme first developed for solvation free energy calculations [20]. The standard form of this correction scheme uses the RISM computed Gaussian fluctuation (GF) free energy and the partial molar volume of a solute as:

$$\Delta G_{\mathrm{corrected}} = \Delta G_{\mathrm{RISM\text{-}GF}} + a^{*}\mathrm{PMV} + b.$$

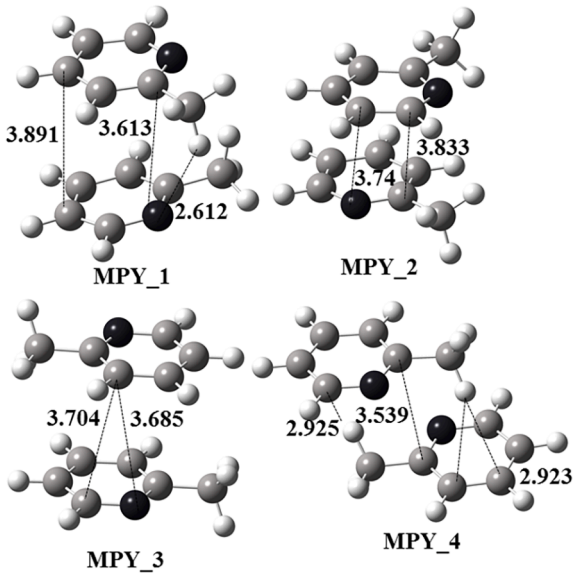

Fig. 6. SMD/B3LYP-D3/cc-pVTZ optimized geometries of the top four dimers of 2-Methylpyridine (MPY). Interatomic distances are in Å. Atom color code: C, grey; H, white; N, black.

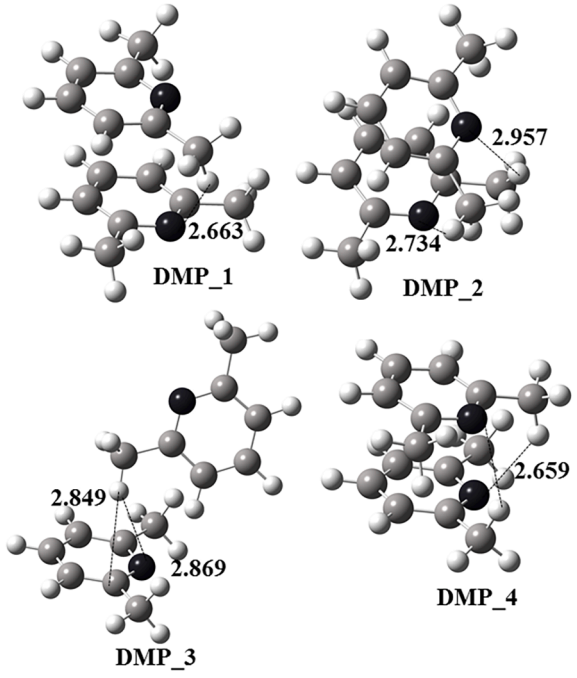

Fig. 7. SMD/B3LYP-D3/cc-pVTZ optimized geometries of the top four dimers of 2,6-Dimethylpyridine (DMP). Interatomic distances are in Å. Atom color code: C, grey; H, white; N, black.

The coefficients *a* and *b* are obtained from linear regression analysis and have units of kcal•mol^{-1}•A^{-3} and kcal•mol^{-1}, respectively. Evidently, a better calibration for solvation free energy through RISM calculations depends on the quality and quantity of data points used in benchmarking.

It is interesting to note that in the polarizable continuum models (PCM) of continuum solvation, the solvation free energy is partitioned into different contributions as:

$\Delta G_{solvation} = \Delta G_{electrostatic} + G_{cavitation} + G_{dispersion} + G_{repulsion} + \Delta G_{molecular\text{-}motion}$.

The dispersion term involves solute–solvent dispersion interactions.

Table 3
Dimerization energetics (in kcal/mol) of the top dimers of aniline (ANL), pyridine (PYR), 2-methylpyridine (MPY), and 2,6-dimethylpyridine (DMP) computed at the SMD/B3LYP-D3/cc-pVTZ level of theory.

System	ΔE	ΔH	ΔG
ANL2_1	−4.84	−4.22	4.02
ANL2_2	−4.97	−4.41	4.97
ANL2_3	−5.96	−5.27	4.19
ANL2_4	−4.80	−4.12	4.59
PYR_1	−2.34	−1.58	6.44
PYR_2	−2.91	−2.08	5.41
PYR_3	−2.92	−2.07	5.17
PYR_4	−2.95	−2.09	4.28
MPY_1	−4.29	−3.70	6.44
MPY_2	−3.88	−3.21	6.23
MPY_3	−3.86	−3.18	6.13
MPY_4	−3.87	−3.21	5.99
DMP_1	−5.00	−4.39	5.73
DMP_2	−3.51	−2.66	5.47
DMP_3	−4.71	−4.07	4.96
DMP_4	−4.96	−4.28	5.32

In general, the electrostatic term is the largest in continuum models. The solute–solvent interaction is described in the PCM model via apparent surface charges spread on the solute cavity by means of treating the electrostatic interactions between the solute wavefunction with the dielectric of solvent. The solute wave function (or electron density) is obtained at a desired quantum level, whereas a set of surface charges on the cavity represents the bulk dielectric model of the solvent [21,22]. The SMD (Solvation Model based on Density) continuum solvation model incorporated the electronic-nuclear-polarization (ENP) energy term and the cavitation/dispersion/solvent-structure (CDS) term. The first one arises from the assumption that the solute structure remains unchanged between the gas phase and bulk. The semi-empirical CDS term accounts for the short range interactions in solvent [23,24].

Computational methods

Molecular dynamics (MD) simulations

All the molecular dynamics simulations were performed using the GROMACS molecular dynamics engine [25]. The liquid aromatic amines were simulated using the all-atom GAFF force field parameters [26,27]. The initial solvent boxes of 256 amine molecules were equilibrated at temperature 298 K and pressure 1 bar using NVT and NPT equilibrium using a Berendsen thermostat without any restraints. A 10 ns production simulation was performed on the equilibrated systems. The molecular (and atomic) distribution functions were computed from the production simulations using the standard utility codes provided in the GROMACS suite.

3D-RISM-KH calculations

The 3D-RISM calculations were performed on the lowest energy conformation of all the solutes generated using the OpenBabel toolkit with the MMFF94 force field [28]. The solutes were parameterized with the GAFF force field with the AM1-BCC charges. The 3D-RISM-KH based excess chemical potential and partial molar volume (used as descriptors in the prediction) were calculated using our in-house code, a working version of which is available in the AMBERTOOLS suite of programs [29]. The united atom AMBER force field parameter was used for the liquid solvents with the AM1-BCC charges [30,31]. The force field parameters used for the RISM calculations are provided in Table 1. The partial atomic charges of all non-aromatic hydrogens are summed to that of the carbon atom to which the H-atom(s) are directly bonded. The extended-RISM (X-RISM) formalism was used for calculating the susceptibility functions of aniline and three pyridines [32].

Table 4
Solvation free energy (SFE in kcal/mol) computed using the CPCM/M06-2X/Def2-TZVPP, SMD/M06-2X/Def2-TZVPP, and 3D-RISM-KH methods.

Solute	Solvent	SFE(exptl.)[a]	SFE(CPCM)	SFE(SMD)	SFE(RISM)
n-octane	dimethylpyridine	−4.88	−0.58	−4.81	−2.97
Toluene	dimethylpyridine	−5.03	−1.18	−4.88	−4.66
Ethanol	dimethylpyridine	−4.87	−2.81	−3.89	−5.47
1,4-dioxane	dimethylpyridine	−4.9	−3.07	−5.45	−6.90
2-butanone	dimethylpyridine	−4.34	−1.97	−5.24	−5.41
2,6-dimethylpyridine	dimethylpyridine	−6.04	−2.71	−5.73	−5.46
n-octane	pyridine	−4.5	−0.63	−4.89	0.06
Toluene	pyridine	−5.1	−1.32	−5.43	−3.06
Ethanol	pyridine	−5.08	−3.04	−4.05	−4.75
1,4-dioxane	pyridine	−5.14	−3.32	−5.62	−5.76
2-butanone	pyridine	−4.61	−2.28	−5.59	−4.15
Pyridine	pyridine	−5.47	−3.11	−6.15	−5.11
Nitromethane	pyridine	−5.11	−5.33	−5.94	−6.28
n-octane	aniline	−3.48	−0.58	−3.98	−1.05
Toluene	aniline	−4.57	−1.17	−4.13	−4.35
Ethanol	aniline	−4.45	−2.79	−4.29	−5.90
1,4-dioxane	aniline	−5.65	−3.05	−4.61	−7.00
2-butanone	aniline	−4.87	−2.91	−4.25	−5.52
Aceticacid	aniline	−6.3	−4.16	−5.30	−7.62
Propanoicacid	aniline	−6.2	−3.89	−5.75	−7.19
Aniline	aniline	−7.61	−3.70	−6.58	−7.46
Nitromethane	aniline	−5.11	−4.88	−3.78	−6.81
Hydrogenperoxide	aniline	−7.8	−4.15	−7.48	−8.29
MAD[b]			**2.56**	**0.63**	**1.17**
RMSE[c]			**2.78**	**0.72**	**1.52**

[a]Experimental solvation free energy from the MNSol database. [b]Mean absolute deviation calculated as: $MAD = \frac{1}{n}\sum_1^n |x_i - x|$. [c]Relative mean square error calculated as: $RMSE = \sqrt{\frac{\sum_1^n (x_i - x)^2}{n}}$; x_i = Predicted free energy, x = Experimental free energy for n-samples.

Density functional theory (DFT) calculations

The dimeric forms of liquid aromatics were explored using the dispersion corrected density functional theory. The B3LYP density functional with the dispersion correction scheme of Grimme and co-workers (B3LYP-D3) was used for calculating the dimer structures of amines with the correlation consistent cc-pVTZ basis set [33–37]. The solvation frees energy calculations were done at the M06-2X/Def2-TZVPP level of theory [38–39]. All the structures were confirmed as minima on the respective potential energy surfaces through vibrational modes analysis, unless noted otherwise. The liquid continua were incorporated for all the DFT calculations using the conductor-like polarizable continuum model (CPCM) and the Minnesota solvation model (SMD) as implemented in the Gaussian16 suite of quantum chemical programs [40–45,51]. The default setting of the CPCM model uses scaled UFF radii to a generate solvent cavity. The SMD solvent model, on the other hand, uses scaled Bondi atomic radii for cavity generation. The effect of the theoretical levels used with the continuum solvation models were tested by further calculating the solvation free energies using the B3LYP functional and at the Hartree-Fock (HF) level in combination with the Def2-TZVPP basis set [33,34,46]. All the reported energies include the zero-point correction.

Results and discussion

The MD equilibration profile of the four pure liquids reported here showed reliable density profiles simulated using the all-atom GAFF force field parameters (Table 2). The radial distribution functions are indicative of the nature of the interactions present in the liquid form. The aniline (ANL) molecules have intermolecular interactions via N•••H(N) and N•••H(C) interactions, as evident from the g_{NH} and g_{NC} radial distribution function (rdf) peaks in the region of ~ 2.5 to 5.5 Å. The multiple peaks are due to possible different molecular orientations leading to H-bonding interactions. Such interactions are also present in the RISM-KH profile (Fig. 2). The RISM profile is indicative of a shorter intermolecular interaction for N•••H(N) H bonding than N•••H(C) interaction, as evident from the position of the maxima in the pair distribution functions (pdfs, Fig. 2).

The atomic distribution functions of pyridines provided interesting information on the molecular arrangements in the liquid form. The N•••N rdfs has a maximum ~ 4.7 Å for PYR, while the same are shifted to a higher separation, ~6 Å, for methylated pyridines, presumably due to steric factors. This feature is very well reproduced by the RISM-KH calculations (Fig. 3). The N•••H interatomic distribution has a sharp maximum at ~ 2 Å for liquid pyridine (PYR) and 2-Methylpyridine (2MP), which is absent for 2,6-Dimethylpyridine (DMP). Multiple peaks are observed between 3 and 6 Å for all three pyridines. The RISM profile of the N•••H interaction differs significantly from the MD rdfs of pyridines by the absence of the peak around 2 Å, instead it is shifted to 3 Å, followed by a hump around 6 Å. The effect can be a result of using united atom force field for the methyl and dimethyl pyridines. An earlier study of the liquid pyridine using diffraction, OPLS force field based MD, and RISM reported heavy atom distributions similar to those reported here [49].

The electronic structure calculations of the four liquids obtained using the dispersion corrected DFT and continuum SMD model yielded dimers stabilized by H-bonding, π-stacking, and X-H•••π interactions. For example, the liquid ANL dimers are stabilized by N•••H(N) interactions with interatomic separation in the range of 2.18–2.23 Å, and N•••H(C) interactions with interatomic separation of 2.63 Å. The (N)H•••π and (C)H•••π interactions were found to have interatomic separations in the range of 2.7–3.0 Å (Fig. 4). These interatomic separations are comparable to the maxima on the corresponding distribution profiles obtained from MD and RISM calculations. The dimerization enthalpy in the liquid phase is found to be in the range of 5.3–4.2 kcal/mol. The PYR dimers in the liquid state has significant π-stacking and C-H•••π interactions (Fig. 5). The dimerization enthalpy of the most stable dimeric form is 2.09 kcal/mol and has a parallel displaced π-stacked geometry. The MPY and DMP dimers in neat liquid have additional $[C_{sp3}]$H•••π interactions along with N•••H H-bonds and other π-cloud involving

interactions (Figs. 6 and 7). These additional interactions impart a larger stabilization enthalpy of the dimers in comparison to PYR liquid dimers. The dimerization computed using DFT-D3 is provided in Table 3.

We have used experimental solvation free energy (SFE) of solutes in aniline, pyridine, 2-methylpyridine, and 2,6-dimethylpyridine from the MNSol database [47,48,50,51]. This dataset is also used to train the SMD solvation model. During the 3D-RISM-KH calculations in the 2-methylpyridine solvent, we have observed some negative PMVs of the solutes, and hence we have not used this solvent for the 3D-RISM SFE calculations. The remaining SFEs in three solvents were calibrated together. Among the atomic surface charge-based continuum models, the CPCM model has the highest mean absolute deviation (MAD) of 2.56 kcal/mol from the experimental benchmarks. The SMD solvation model, on the other hand, has the best performance with a MAD of 0.63 kcal/mol. The UC-corrected SFEs from the 3D-RISM-KH has a slightly worse performance than SMD model, but outperforms the CPCM computed SFEs with a MAD of 1.17 kcal/mol. All the computed SFEs are provided in Table 4. The effect of the level of theory in calculating the SFEs using the QM continuum models are found to be negligible. (Footnote 1).

Conclusion

In this work, we have extended the 3D-RISM-KH molecular solvation theory to explore the liquid state of four aromatic compounds: aniline, pyridine, 2-methylpyridine, and 2,6-dimethylpyridine. The liquid states of these compounds have ordered structures owing to N···H hydrogen bonding, NH···π, CH···π, and π-stacking interactions. These observations have been further supported from the electronic structure calculations using DFT-D3 theory. The 3D-RISM-KH theory computed SFEs are at par with those computed using the SMD solvation models, although the former requires much less computational resources.

Declaration of Competing Interest

The authors declare that they have no known competing financial interests or personal relationships that could have appeared to influence the work reported in this paper.

Acknowledgements:

This work was financially supported by the NSERC Discovery Grant (RES0029477), and Canadian Consortium on Neurodegeneration in Aging (CCNA) Protein Misfolding, Phase II Grant (RES0051206). Generous computing time provided by WestGrid (www.westgrid.ca) and Compute Canada/Calcul Canada (www.computecanada.ca) is acknowledged.

Appendix A. Supplementary data

Supplementary data to this article can be found online at https://doi.org/10.1016/j.rechem.2022.100365.

References:

[1] A. Plugatyr, I.M. Svishchev, The hydration of aniline: Analysis of spatial distribution functions, J. Chem. Phys. 130 (11) (2009) 114509, https://doi.org/10.1063/1.3096672.
[2] M. Nagasaka, H. Yuzawa, N. Kosugi, Intermolecular Interactions of Pyridine in Liquid Phase and Aqueous Solution Studied by Soft X-ray Absorption Spectroscopy, Z. Phys. Chem. 232 (2008) 705–722, https://doi.org/10.1515/zpch-2017-1054.
[3] P.E. Mason, G.W. Neilson, C.E. Dempsey, D.L. Price, M.-L. Saboungi, J.W. Brady, Observation of pyridine aggregation in aqueous solution using neutron scattering experiments and MD simulations, J. Phys. Chem. B 114 (16) (2010) 5412–5419, https://doi.org/10.1021/jp9097827.
[4] M.H. Ghatee, A.R. Zolghadr, F. Moosavi, L. Pakdel, The extent of molecular orientation at liquid/vapor interface of pyridine and its alkyl derivatives by molecular dynamics simulation, J. Chem. Phys. 134 (7) (2011) 074707, https://doi.org/10.1063/1.3554361.
[5] W. Marczak, K. Kiełek, B. Czech, H. Flakus, M. Rogalski, Complexes of 2,6-dimethylpyridine with water in condensed phases and the dynamical co-operative interactions involving hydrogen bonds, Phys. Chem. Chem. Phys. 11 (2009) 2668–2678, https://doi.org/10.1039/B818747A.
[6] G.S. Kürkçüoğlu, I. Kavlak, T. Arslan, C. Öğretir, Theoretical studies on the molecular structure and vibrational spectra of some dimethyl substituted pyridine derivatives, J. Mol. Model. 15 (1) (2009) 79–90, https://doi.org/10.1007/s00894-008-0368-y.
[7] N.P. Funnell, A. Dawson, W.G. Marshall, S. Parsons, Destabilisation of hydrogen bonding and the phase stability of aniline at high pressure, CrystEngComm 15 (6) (2013) 1047–1060, https://doi.org/10.1039/C2CE26403J.
[8] S. Crawford, M. Kirchner, D. Bläser, R. Boese, W.F. David, A. Dawson, A. Gehrke, R. Ibberson, W. Marshall, S. Parsons, O. Yamamuro, Isotopic Polymorphism in Pyridine, Angew. Chem. Int. Ed. 48 (4) (2009) 755–757, https://doi.org/10.1002/anie.200803589.
[9] E. Castellucci, G. Sbrana, F.D. Verderame, J. Chem. Phys. 51 (1969) 3762, https://doi.org/10.1063/1.1672590.
[10] A.D. Bond, J.E. Davies, 2-Picoline, Acta Cryst. E 57 (11) (2001) o1089–o1090, https://doi.org/10.1107/S1600536801017548.
[11] A.D. Bond, J.E. Davies, A.J. Kirby, 2,6-Lutidine, Acta Cryst. E 57 (12) (2001) o1242–o1244, https://doi.org/10.1107/S1600536801019869.
[12] D. Chandler, H.C. Andersen, Optimized cluster expansions for classical fluids. II. Theory of molecular liquids, J. Chem. Phys. 57 (5) (1972) 1930–1937, https://doi.org/10.1063/1.1678513.
[13] D. Chandler, Derivation of an integral equation for pair correlation functions in molecular fluids, J. Chem. Phys. 59 (5) (1973) 2742–2746, https://doi.org/10.1063/1.1680393.
[14] D. Chandler, J.D. McCoy, S.J. Singer, Density functional theory of nonuniform polyatomic systems. I. General formulation, J. Chem. Phys. 85 (10) (1986) 5971–5976, https://doi.org/10.1063/1.451510.
[15] D. Chandler, J.D. McCoy, S.J. Singer, Density functional theory of nonuniform polyatomic systems. II. Rational closures for integral equations, J. Chem. Phys. 85 (10) (1986) 5977–5982, https://doi.org/10.1063/1.451511.
[16] D. Chandler, Equilibrium structure and molecular motion in liquids, Acc. Chem. Res. 7 (8) (1974) 246–251, https://doi.org/10.1021/ar50080a002.
[17] A. Kovalenko, Molecular theory of solvation: Methodology summary and illustrations, Cond. Matt. Phys. 18 (2015) 32601, https://doi.org/10.5488/CMP.18.32601.
[18] D. Roy, A. Kovalenko, 3D-RISM-KH Molecular Solvation Theory, in: D.R. Salahub, D. Wei (Eds.).
[19] Multiscale Dynamics Simulations: Nano and Nano-bio Systems in Complex Environments, RSC Publishing, London, 2021, pp. 254–286. https://doi.org/10.1039/9781839164668-00254.
[20] A. Kovalenko, F. Hirata, Potential of mean force between two molecular ions in a polar molecular solvent: A study by the three-dimensional reference interaction site model, J. Phys. Chem. B 103 (1999) 7942–7957, https://doi.org/10.1021/jp991300+.
[21] D.S. Palmer, A.I. Frolov, E.L. Ratkova, M.V. Fedorov, Towards a universal method for calculating hydration free energies: a 3D reference interaction site model with partial molar volume correction, J Phys Condens Matter. 22 (49) (2010) 492101, https://doi.org/10.1088/0953-8984/22/49/492101.
[22] B. Mennucci, Polarizable continuum model, WIRES Comput. Mol. Sci. 2 (3) (2012) 386–404, https://doi.org/10.1002/wcms.1086.
[23] J. Tomasi, Selected features of the polarizable continuum model for the representation of solvation, WIRES Comput. Mol. Sci. 1 (5) (2011) 855–867, https://doi.org/10.1002/wcms.54.
[24] A.V. Marenich, C.J. Cramer, D.G. Truhlar, Perspective on Foundations of Solvation Modeling: The Electrostatic Contribution to the Free Energy of Solvation, J. Chem. Theory Comput. 4 (6) (2008) 877–887, https://doi.org/10.1021/ct800029c.
[25] C.J. Cramer, D.G. Truhlar, A Universal Approach to Solvation Modeling, Acc. Chem. Res. 41 (6) (2008) 760–768, https://doi.org/10.1021/ar800019z.
[26] M.J. Abraham, T. Murtola, R. Schulz, S. Páll, J.C. Smith, B. Hess, E. Lindahl, GROMACS: High performance molecular simulations through multi-level parallelism from laptops to supercomputers, SoftwareX 1–2 (2015) 19–25, https://doi.org/10.1016/j.softx.2015.06.001.
[27] J. Wang, W. Wang, P.A. Kollman, D.A. Case, Automatic atom type and bond type perception in molecular mechanical calculations, J. Mol. Graph. Model. 25 (2) (2006) 247–260, https://doi.org/10.1016/j.jmgm.2005.12.005.
[28] J. Wang, R.M. Wolf, J.W. Caldwell, P.A. Kollman, D.A. Case, Development and testing of a general amber force field, J. Comput. Chem. 25 (9) (2004) 1157–1174, https://doi.org/10.1002/jcc.v25:910.1002/jcc.20035.
[29] N.M. O'Boyle, M. Banck, C.A. James, C. Morley, T. Vandermeersch, G. R. Hutchison, Open Babel: An open chemical toolbox, J. Cheminform. 3 (2011) 33, https://doi.org/10.1186/1758-2946-3-33.
[30] D.A. Case, H.M. Aktulga, K. Belfon, I.Y. Ben-Shalom, S.R. Brozell, D.S. Cerutti, T.E. Cheatham, III, V.W.D. Cruzeiro, T.A. Darden, R.E. Duke, G. Giambasu, M.K. Gilson, H. Gohlke, A.W. Goetz, R. Harris, S. Izadi, S.A. Izmailov, C. Jin, K. Kasavajhala, M. C. Kaymak, E. King, A. Kovalenko, T. Kurtzman, T.S. Lee, S. LeGrand, P. Li, C. Lin, J. Liu, T. Luchko, R. Luo, M. Machado, V. Man, M. Manathunga, K.M. Merz, Y. Miao, O. Mikhailovskii, G. Monard, H. Nguyen, K.A. O'Hearn, A. Onufriev, F. Pan, S. Pantano, R. Qi, A. Rahnamoun, D.R. Roe, A. Roitberg, C. Sagui, S. Schott-Verdugo, J. Shen, C.L. Simmerling, N.R. Skrynnikov, J. Smith, J. Swails, R.C. Walker, J. Wang, H. Wei, R.M. Wolf, X. Wu, Y. Xue, D.M. York, S. Zhao, P.A. Kollman, Amber 2021, University of California, San Francisco.

[31] L. Yang, C.-h. Tan, M.-J. Hsieh, J. Wang, Y. Duan, P. Cieplak, J. Caldwell, P. A. Kollman, R. Luo, New-Generation Amber United-Atom Force Field, J. Phys. Chem. B 110 (26) (2006) 13166–13176, https://doi.org/10.1021/jp060163v.
[32] A. Jakalian, D.B. Jack, C.I. Bayly, Fast, efficient generation of high-quality atomic charges. AM1-BCC model: II. Parameterization and validation, J. Comput. Chem. 23 (2002) 1623–1641, https://doi.org/10.1002/jcc.10128.
[33] Fumio Hirata, Peter J. Rossky, An extended rism equation for molecular polar fluids, Chem. Phys. Lett. 83 (2) (1981) 329–334, https://doi.org/10.1016/0009-2614(81)85474-7.
[34] A.D. Becke, Density-functional exchange-energy approximation with correct asymptotic-behavior, Phys. Rev. A 38 (6) (1988) 3098–3100.
[35] C. Lee, W. Yang, R.G. Parr, Development of the Colle-Salvetti correlation-energy formula into a functional of the electron density, Phys. Rev. B 37 (1988) 785–789.
[36] S. Grimme, J. Antony, S. Ehrlich, H. Krieg, A consistent and accurate ab initio parameterization of density functional dispersion correction (DFT-D) for the 94 elements H-Pu, J. Chem. Phys. 132 (2010), 154104, https://doi.org/10.1063/1.3382344.
[37] Thom H. Dunning, Gaussian basis sets for use in correlated molecular calculations. I. The atoms boron through neon and hydrogen, J. Chem. Phys. 90 (2) (1989) 1007–1023, https://doi.org/10.1063/1.456153.
[38] D.E. Woon, T.H. Dunning Jr., Gaussian-basis sets for use in correlated molecular calculations. 3. The atoms aluminum through argon, J. Chem. Phys. 98 (1993) 1358–1371, https://doi.org/10.1063/1.464303.
[39] Yan Zhao, Donald G. Truhlar, The M06 suite of density functionals for main group thermochemistry, thermochemical kinetics, noncovalent interactions, excited states, and transition elements: two new functionals and systematic testing of four M06-class functionals and 12 other functionals, Theor. Chem. Acc. 120 (1-3) (2008) 215–241, https://doi.org/10.1007/s00214-007-0310-x.
[40] F. Weigend, R. Ahlrichs, Balanced basis sets of split valence, triple zeta valence and quadruple zeta valence quality for H to Rn: Design and assessment of accuracy, Phys. Chem. Chem. Phys. 7 (2005) 3297–3305, https://doi.org/10.1039/B508541A.
[41] Jacopo Tomasi, Benedetta Mennucci, Roberto Cammi, Quantum mechanical continuum solvation models, Chem. Rev. 105 (8) (2005) 2999–3094, https://doi.org/10.1021/cr9904009.
[42] J. Tomasi, B. Mennucci, E. Cancès, The IEF version of the PCM solvation method: An overview of a new method addressed to study molecular solutes at the QM ab initio level, J. Mol. Struct. (Theochem) 464 (1-3) (1999) 211–226, https://doi.org/10.1016/S0166-1280(98)00553-3.
[43] Vincenzo Barone, Maurizio Cossi, Jacopo Tomasi, A new definition of cavities for the computation of solvation free energies by the polarizable continuum model, J. Chem. Phys. 107 (8) (1997) 3210–3221, https://doi.org/10.1063/1.474671.
[44] M. Cossi, V. Barone, R. Cammi, J. Tomasi, Ab initio study of solvated molecules: A new implementation of the polarizable continuum model, Chem. Phys. Lett. 255 (1996) 327–335, https://doi.org/10.1063/1.474671.
[45] A.V. Marenich, C.J. Cramer, D.G. Truhlar, Universal solvation model based on solute electron density and a continuum model of the solvent defined by the bulk dielectric constant and atomic surface tensions, J. Phys. Chem. B 113 (2009) 6378–6396, https://doi.org/10.1021/jp810292n.
[46] Gaussian 16, Revision C.01, M. J. Frisch, G. W. Trucks, H. B. Schlegel, G. E. Scuseria, M. A. Robb, J. R. Cheeseman, G. Scalmani, V. Barone, G. A. Petersson, H. Nakatsuji, X. Li, M. Caricato, A. V. Marenich, J. Bloino, B. G. Janesko, R. Gomperts, B. Mennucci, H. P. Hratchian, J. V. Ortiz, A. F. Izmaylov, J. L. Sonnenberg, D. Williams-Young, F. Ding, F. Lipparini, F. Egidi, J. Goings, B. Peng, A. Petrone, T. Henderson, D. Ranasinghe, V. G. Zakrzewski, J. Gao, N. Rega, G. Zheng, W. Liang, M. Hada, M. Ehara, K. Toyota, R. Fukuda, J. Hasegawa, M. Ishida, T. Nakajima, Y. Honda, O. Kitao, H. Nakai, T. Vreven, K. Throssell, J. A. Montgomery, Jr., J. E. Peralta, F. Ogliaro, M. J. Bearpark, J. J. Heyd, E. N. Brothers, K. N. Kudin, V. N. Staroverov, T. A. Keith, R. Kobayashi, J. Normand, K. Raghavachari, A. P. Rendell, J. C. Burant, S. S. Iyengar, J. Tomasi, M. Cossi, J. M. Millam, M. Klene, C. Adamo, R. Cammi, J. W. Ochterski, R. L. Martin, K. Morokuma, O. Farkas, J. B. Foresman, D. J. Fox, Gaussian 16, rev. B.01, Gaussian, Inc., Wallingford CT, 2016.
[47] C.C.J. Roothaan, New Developments in Molecular Orbital Theory, Rev. Mod. Phys. 23 (2) (1951) 69–89, https://doi.org/10.1103/RevModPhys.23.69.
[48] W.M. Haynes (Ed.), CRC Handbook of Chemistry and Physics, 95th ed., CRC Press Inc., Florida, 2014–2015..
[49] S. Budavari,(ed.), The Merck Index - An Encyclopedia of Chemicals, Drugs, and Biologicals. Whitehouse Station, NJ: Merck and Co., Inc., 1996.
[50] I. Bakó, T. Radnai, G. Pálinkás, Investigation of the Structure of Liquid Pyridine: a Molecular Dynamics Simulation, an RISM, and an X-ray Diffraction Study, Z. Naturforsch. 51a (1996) 859-866. https://doi.org/10.1515/zna-1996-0710.
[51] A.V. Marenich, C.P. Kelly, J.D. Thompson, G.D. Hawkins, C.C. Chambers, D.J. Giesen, P. Winget, C.J. Cramer, D.G. Truhlar, Minnesota Solvation Database (MNSOL) version 2012.